

Kinetic Energy Management with Surrounding Vehicles Behavior Prediction *

Yutaro ITOH

Hiroyuki NANJO

Mitsuharu HIGASHITANI

Daisuke HIRANO

Kazuhito TAKENAKA

This paper explains a novel adaptive cruise control (ACC) driving with coasting to improve fuel economy. The purpose is to reduce the energy loss with predictive control when the preceding vehicle decelerates, while an acceptable driving feeling is guaranteed. To achieve this goal, the prediction of the preceding vehicle behavior is introduced to determine the ego vehicle behavior realized by using inverse reinforcement learning (IRL). Besides, the cost function is designed to determine the optimal coasting timing by balancing longer coasting time and an acceptable driving feeling, while the ego vehicle speed is controlled with a rule-based control at a non-coasting period. The performance of this control strategy has been validated with simulation, showing a 9.7% fuel economy improvement on average for hybrid electric vehicles in the case of following the preceding vehicle before an intersection. It has also been validated with an actual test vehicle, where a high-level balance between high efficiency and an acceptable feeling is realized.

Key words :

energy management, ADAS, predictive control, probabilistic prediction

1. Introduction

Recently, advanced driver assistance systems (ADAS) have been actively developed to improve safety and convenience. ADAS is the technology controlling vehicle behavior with the surrounding environment information such as adaptive cruise control (ACC) or lane change assist (LCA). By using these technologies, fuel economy can also be improved drastically¹⁾⁻⁴⁾.

Fig. 1 shows our perspective of energy management technology ranging from level 1 to 4. Level 1 is

“in-car energy management”. Level 2 is “predictive energy management” such as predictive ACC. Level 3 is “energy management for passenger and freight transport”, where transportation companies reduce their CO₂ emissions. Finally, level 4 is “energy management in a smart city”. In this paper, as a solution at level 2, predictive ACC to reduce CO₂ emissions drastically, namely ECO ACC, is introduced.

This paper is organized as follows: section 2 presents the overview of ECO ACC and its technical issues.

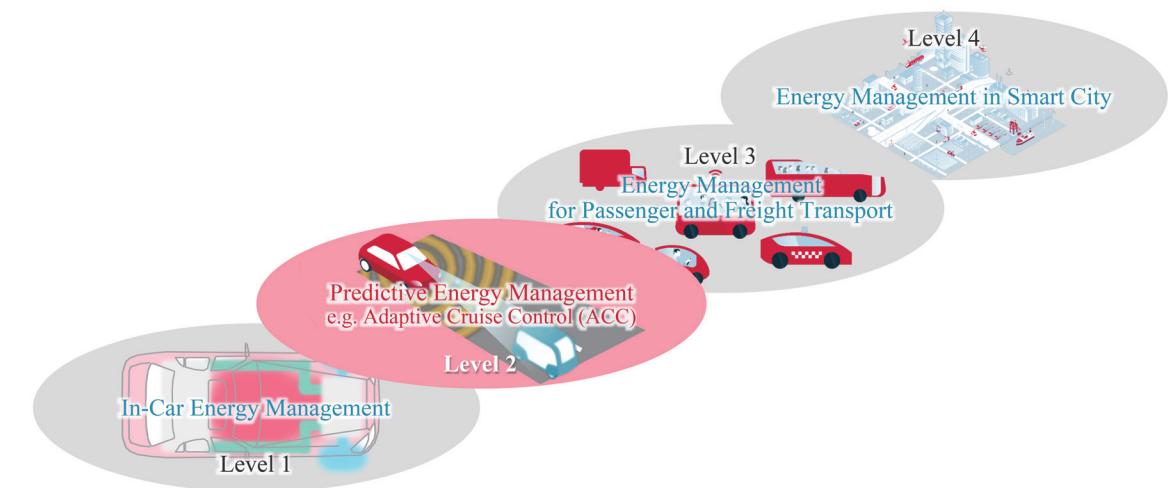


Fig. 1 Our perspective of energy management technology

The prediction technology used for ECO ACC is described in section 3. In section 4, the control scheme and the design of ECO ACC are described. Afterward, the validation results based on a simulation and a test vehicle provided in section 5 shows the performance of the proposed control strategy in the real world. Lastly, the conclusion and future work are given in section 6.

2. Overview of “ECO ACC” and Issues

To improve fuel economy, the following three methods are effective: shifting the driving point to improve efficiency, decreasing the maximum vehicle speed to reduce road load, and utilizing kinetic energy as much as possible to minimize energy loss. In city driving, fuel economy can be improved mainly when decelerating before an intersection. In this situation, these three methods are realized with additional engine stop driving, lower vehicle speed, and extending driving distance with kinetic energy. This driving pattern known as coasting can improve fuel economy drastically. Therefore, we use coasting as a main efficient driving way for our ECO ACC.

When the ego vehicle follows the preceding vehicle, we can define an ideal driving condition of the ego

vehicle represented with time headway (THW). It is determined by the safety requirement and the following performance. With ECO ACC, the ego vehicle uses coasting in or around this condition as much as possible. However, when the preceding vehicle decelerates or an adjacent vehicle cuts in, the ego vehicle needs to decelerate as well to avoid collision depending on the situation. If unnecessary preceding vehicle following is avoided, energy loss can be reduced by lower vehicle speed. Fig. 2 shows a result example in which fuel economy deteriorates by 80% mainly due to the energy loss of unnecessary driving to follow the preceding vehicle. While the vehicle drives with coasting in the ideal case, the preceding vehicle behavior is copied by the ego vehicle in the actual case. (Driving condition: following the preceding vehicle before an intersection, test vehicle: C-segment hybrid electric vehicle (HEV), engine displacement: 2L.) In this paper, we aim to improve fuel economy by reducing the energy loss due to unnecessary preceding vehicle following under the condition that an acceptable driving feeling is maintained.

To realize this goal, we introduce a prediction technology of the surrounding vehicle behavior to decide the optimal coasting timing. In this paper, we focus on the deceleration of the preceding vehicle,

* (公社)自動車技術会の了解を得て、2019年秋季大会学術講演会 講演予稿集 No.105-19 p.1 ~ 文献番号: 20196069 より修正・加筆し転載

although the method that we use can also be applied for other vehicle behavior such as the cut-in of an adjacent vehicle. Here, since it is almost impossible to predict the preceding vehicle behavior with 100% accuracy, the predicted result includes uncertainty represented with probability. By using the prediction information, the coasting timing is derived by solving an optimization problem to manage both fuel economy improvement and driving feeling guarantee.

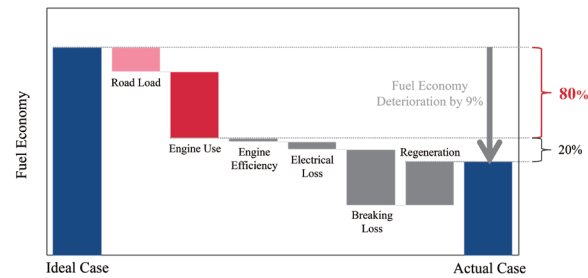


Fig. 2 Fuel economy comparison between ideal case with coasting and actual case

3. Prediction Technology Introduction

3.1 Overview of Inverse Reinforcement Learning

In this paper, inverse reinforcement learning (IRL)⁵⁾ is used to predict vehicle behavior. IRL is one of the imitation learning methods of behavior from demonstrations. By using the framework, future vehicle behavior can be predicted as mentioned in⁶⁾. In this method, a reward function is learned from demonstrations in Markov Decision Process (MDP) framework. An agent performs actions to maximize the cumulative reward defined with the reward function. The future behavior can be predicted as a likely action sequence from the current state based on the reward function. Besides, a similarity (likelihood) between a demonstration and histories of behavior (recorded sequences) can also be measured by using the reward function.

3.2 Vehicle Behavior Modeling with IRL

In our case, we first classify vehicle behavior demonstrations represented with the vehicle position, speed, and acceleration before an intersection into two categories: stopping and passing behavior. Secondly, we individually estimate reward functions from demonstrations in each of the two categories where the vehicle position and speed are modeled as states, and acceleration is modeled as an action in MDP framework. To predict the future behavior of the preceding vehicle based on the current observation, we calculate the likelihood and the optimal action sequence for each of the categories. The likelihood represents the extent to which the observed behavior belongs to each category, and the optimal action (acceleration) sequence represents an expected future behavior if the observed behavior belongs to each category. Both the likelihoods and the optimal action sequences are used for the predictive control mentioned in section 4.

3.3 Applying IRL Result for Prediction Usage

By using the likelihoods, we can calculate probabilistically which category of behavior the preceding vehicle belongs to. For the classification, we focus on the difference between two log likelihoods (log likelihood gap) for stopping and passing behavior. Here, the log likelihood gap $g(\psi)$ is defined as the following equation:

$$g(\psi) = l_{\text{stop}}(\psi) - l_{\text{pass}}(\psi), \quad (1)$$

where $l_{\text{stop}}(\psi)$ and $l_{\text{pass}}(\psi)$ are the log likelihood for stopping and passing behavior, respectively, at the preceding vehicle position ψ . It is assumed that distributions of the log likelihood gap for each category change with the position ψ and that the distributions at each position are Gaussian distribution. Once the distributions of the log likelihood gap are calculated,

the probability value represented with the following equation can be obtained for each category at any time:

$$p(c|g(\psi)) = \frac{N(g(\psi); \mu_c(\psi), \sigma_c(\psi)^2)}{\sum_c N(g(\psi); \mu_c(\psi), \sigma_c(\psi)^2)}. \quad (2)$$

Here, $\mu_c(\psi)$ and $\sigma_c(\psi)$ are the mean and the variance at the position ψ , respectively, when the preceding vehicle behavior belongs to the behavior category c (passing or stopping). Fig. 3 shows an example of log likelihood gap distributions for each category and the stopping behavior appearance probability at each log likelihood gap.

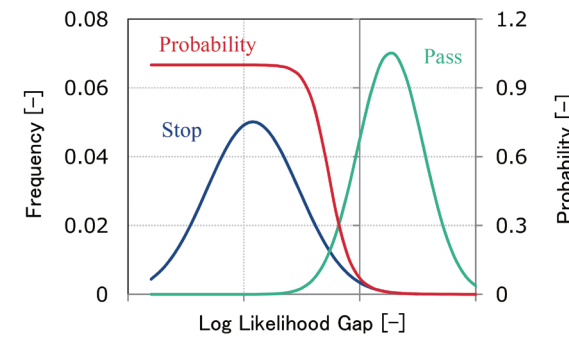


Fig. 3 Stopping behavior appearance probability based on likelihood

4. Vehicle Speed Optimization

4.1 Optimization Problem Formulation

As mentioned in section 2, the energy loss caused by the unnecessary following needs to be reduced to improve fuel economy. On the other hand, the deviation from the ideal driving condition also needs to be reduced to guarantee the following performance. Therefore, the optimization problem should be formulated to fulfill both requirements. Let us consider n types of preceding vehicle behavior with their appearance probability. We can calculate the driving energy of the i -th predicted behavior as follows:

$$\varepsilon_i(v_e(t)) = \int_0^T \pi_i(v_e(t), t) dt \quad (0 \leq i \leq n), \quad (3)$$

where v_e is the ego vehicle speed time sequence, t is the time, T is the time length of behavior, and π_i is the driving power time sequence of the ego vehicle. On the other hand, the deviation from the ideal driving condition is defined as follows:

$$\delta_i(v_e(t)) = \int_0^T y_i(v_e(t), v_p(t), t) dt \quad (0 \leq i \leq n), \quad (4)$$

Here, y_i is the distance from the edge of the ideal driving condition to follow the preceding vehicle expressed as follows:

$$y_i(v_e(t), v_p(t), t) = \begin{cases} d_{\min}(v_e(t), v_p(t), t) - d(v_e(t), v_p(t), t) & (d < d_{\min}) \\ d(v_e(t), v_p(t), t) - d_{\max}(v_e(t), v_p(t), t) & (d > d_{\max}) \\ 0 & (\text{otherwise}) \end{cases} \quad (5)$$

where d_{\min} is the minimum driving distance from the preceding vehicle, d_{\max} is the maximum one, d is the current one, and v_p is the preceding vehicle speed time sequence. If ε_i is minimized, fuel economy is maximized. On the other hand, small δ_i means that the ego vehicle drives in or around the ideal driving condition. Since the preceding vehicle behavior is represented with a probability, both the driving energy and the deviation from the ideal driving condition can be expressed as the following expected values:

$$\varepsilon(v_e(t)) = \sum_{i=1}^n p_i \varepsilon_i(v_e(t)), \quad (6)$$

$$\delta(v_e(t)) = \sum_{i=1}^n p_i \delta_i(v_e(t)), \quad (7)$$

where p_i is the appearance probability of the i -th predicted behavior. By using these two variables, we design the optimization problem as follows:

$$\min_{v_e} \sum_{i=1}^n p_i \{k \varepsilon_i(v_e(t)) + (1-k) \delta_i(v_e(t))\}, \quad (8)$$

where k is a weighting factor whose range of value is $0 \leq k \leq 1$. Our goal is to determine the vehicle speed to minimize this cost function.

4.2 Optimal Condition Derivation

If we can omit unnecessary following behavior of the preceding vehicle, driving patterns of ECO ACC can be represented only with the following phase without braking behavior and the coasting phase. Therefore, assuming that the vehicle can drive with these two phases by optimization, we decide when to start coasting to minimize the cost function. Fig. 4 shows a toy example illustrating three different coasting patterns. If the vehicle starts coasting at an earlier stage, then the THW is increased, which is not preferable in the sense of the following function (#1 shown in Fig. 4). On the other hand, if the vehicle starts coasting at a later stage, then the driving energy is increased to guarantee an appropriate THW, which leads to fuel economy deterioration (#3 shown in Fig. 4). For this problem, the optimization problem Eq. (8) is replaced with the following equation to find the optimal coasting timing (#2 shown in Fig. 4):

$$\min_{\tau} \sum_{i=1}^n p_i \{k\varepsilon_i(\tau) + (1-k)\delta_i(\tau)\}, \quad (9)$$

because the ego vehicle speed v_e is determined by the coasting start timing τ . Since the simplified cost

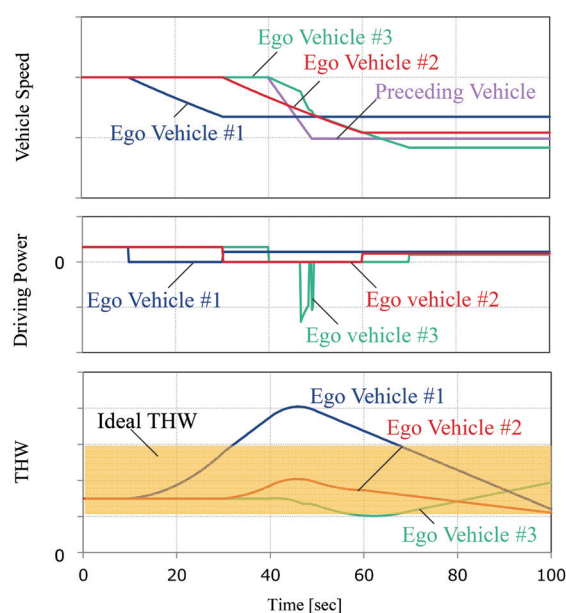


Fig. 4 Vehicle behavior with different coasting timing

function in Eq. (9) is one dimensional, it is easy to identify the optimal condition even by using an exhaustive search. If the vehicle starts coasting when the function value at $\tau = 0$ is minimum, we can achieve the goal.

4.3 Control Scheme

Fig. 5 shows the control framework implemented in the actual test vehicle. The rule-based logic illustrated at the bottom always calculates the target acceleration, which is converted into the target traction force. On the other hand, the coasting command is determined based on the predictive control. When the arbitration block receives the coasting flag, the target traction force is rewritten to zero (i.e. coasting).

With our control strategy, the vehicle speed except in the coasting phase is determined based on the current time headway (THW) and the relative speed. Therefore, after the ego vehicle finishes coasting, where the THW tends to be relatively large, it could accelerate to decrease the THW. Since this behavior causes an increase of the ego vehicle speed, the energy loss to follow the preceding vehicle is also increased, which causes fuel economy deterioration. To solve this problem, an additional function is introduced to suppress unnecessary acceleration based on the prediction information as shown in Fig. 6. Right after the ego vehicle finishes coasting, the target vehicle speed is determined to be a lower value than usual. Let us define the vehicle speed when the vehicle finishes coasting as v_{cst} and the target vehicle speed generated by the rule-based control as $v_{acc}(t)$, respectively. The higher the stopping behavior appearance probability is, the closer to $v_{acc}(t)$ the final target vehicle speed $v_{tag}(t)$ should be. Therefore, $v_{tag}(t)$ is determined with the following equation:

$$v_{tag}(t) = \alpha v_{cst} + (1 - \alpha)v_{acc}(t). \quad (10)$$

Here, α is a function of the stopping behavior

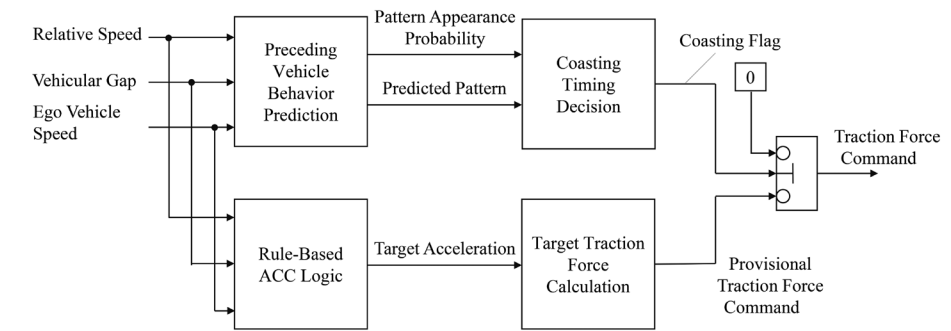


Fig. 5 Control framework implemented in actual test vehicle

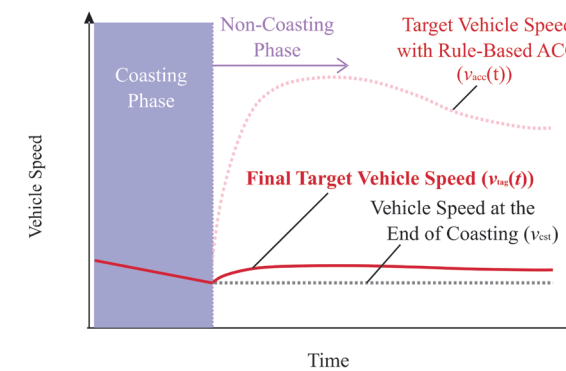


Fig. 6 Image of "unnecessary acceleration suppression function"

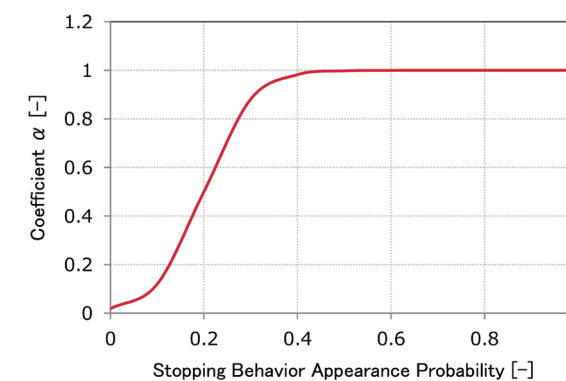


Fig. 7 Coefficient α with respect to stopping behavior appearance probability

appearance probability shown in Fig. 7. Since the vehicle accelerates to catch up with the preceding vehicle after passing through an intersection, the total trip time is not increased so much.

5. Validation

Fuel economy improvement with the developed control strategy mentioned in this paper is validated

with simulation. While the target vehicle speed is determined by the rule-based ACC control strategy, an additional coasting command is generated based on the control strategy mentioned in section 4 with the prediction information of the preceding vehicle behavior. Simulation condition is as follows:

- Simulation vehicle: C-segment HEV
- Engine displacement: 2 L
- Driving condition: following the preceding vehicle before an intersection
- Other condition: ambient temperature = 25°C, hot start

For training and validation, we utilize driving history data in which vehicles drive before an intersection without a traffic signal in Higashiura, Aichi, Japan as shown in Fig. 8. Vehicles driving at this road have two choices: passing through without deceleration and turning right with deceleration. Since there is no traffic signal, the ego vehicle has to predict the preceding vehicle behavior only from the sensing information. The data used for validation are shown in Fig. 9. The distance from the initial point to the terminal point (the intersection) illustrated with an arrow in Fig. 8 is 600 m. All the data are divided into two groups (stopping and passing behavior). Fig. 10 shows a simulation result when the preceding vehicle stops before the intersection. Here, the predicted result of the preceding vehicle is illustrated at intervals of 5 sec. For the actual control, the predicted result of passing behavior, which is not shown in Fig. 10,

is also used. Based on the predicted speed sequences of the preceding vehicle and the stopping behavior appearance probability, the ego vehicle executes coasting from $t = 16$ sec to 20 sec. After that, thanks to the unnecessary acceleration suppression function, the ego vehicle speed is maintained with a lower value in order not to increase the energy loss due to deceleration until $t = 32$ sec. Besides, before the

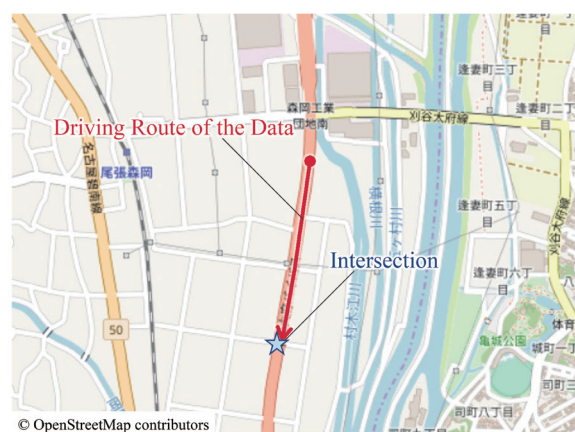


Fig. 8 Driving route

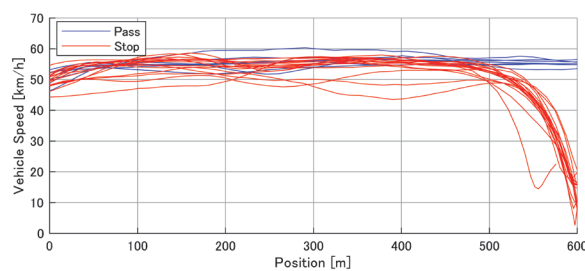


Fig. 9 Actual driving data for verification

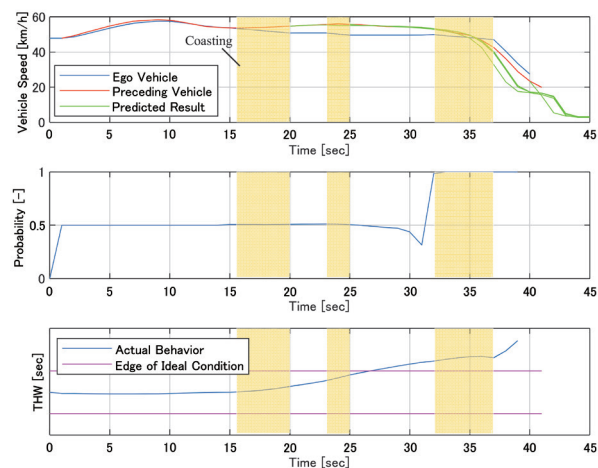


Fig. 10 Time chart of vehicle simulation result (preceding vehicle: stop)

preceding vehicle starts deceleration, the ego vehicle executes coasting again from $t = 32$ sec to $t = 37$ sec. Consequently, fuel economy is improved mainly due to the reduced driving energy. Fig. 11 shows another simulation result when the preceding vehicle passes through the intersection. Because the stopping behavior appearance probability is not low (50%) at $t = 15$ sec, the ego vehicle executes coasting. After that, as with the case of Fig. 10, the unnecessary acceleration suppression and the coasting function maintain the ego vehicle speed until about $t = 30$ sec. However, afterward, due to the low stopping behavior appearance probability and the predicted vehicle speed without both huge acceleration and deceleration, the ego vehicle starts following the preceding vehicle again. In both cases shown in Fig. 10 and Fig. 11, the THW during cruising is controlled in or around the ideal condition.

Fig. 12 shows the simulation result of the amount of fuel economy improvement when the preceding vehicle stops before the intersection. The number of simulation samples is 17. In some cases, fuel economy is improved by more than 20%, where the preceding vehicle does not drive efficiently or the ego vehicle can execute coasting for a long time with an appropriate vehicular gap. Although performance varies depending on the situation, fuel economy is improved in all cases.

In terms of the average value illustrated with a dotted line, a 9.7% fuel economy improvement is achieved. On the other hand, Fig. 13 shows the comparison result between THW distributions with and without the prediction information when the preceding vehicle passes through the intersection. The dotted lines indicate the edge of the ideal condition. The number of simulation samples is seven. The condition sandwiched between two edges is the ideal condition. Although the THW distribution of the control with the prediction technology is shifted to the right side (i.e. larger THW), every case still exists within the

ideal THW range, which indicates that the driving feeling is acceptable.

This control strategy is implemented in the actual test vehicle as shown in Fig. 14. Although the computational cost of the prediction part based on

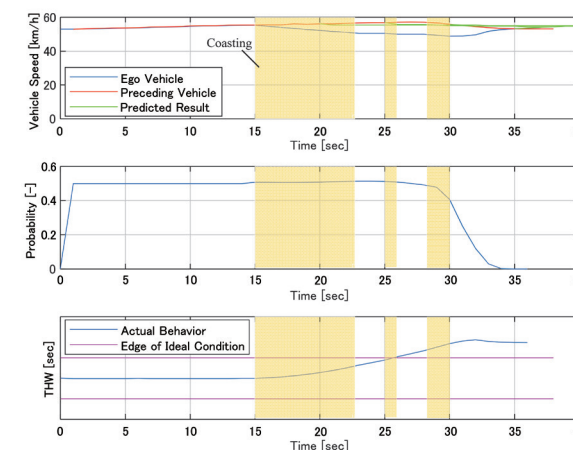


Fig. 11 Time chart of vehicle simulation result (preceding vehicle: pass)

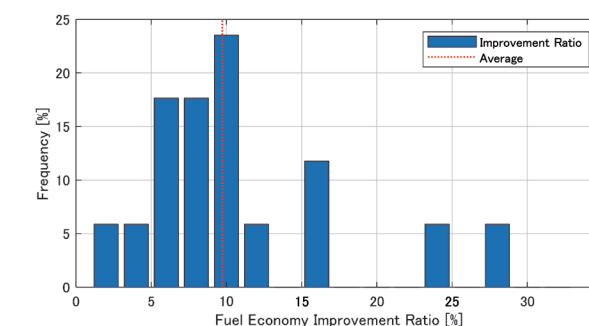


Fig. 12 Histogram of fuel economy improvement value (preceding vehicle: stop)

IRL is low enough to be executed in an ECU installed in an actual vehicle, it is necessary to have a large memory to store the trained information. Therefore, in this time, the function predicting the preceding vehicle behavior and calculating the optimal coasting timing is implemented with Matlab® in the PC. For the mass production phase, it is a future issue. The other part including the rule-based control is installed into the AutoBox®. The control strategy is validated with the same condition as simulation (i.e. following the preceding vehicle before an intersection), where the driving feeling is even better than the conventional ACC due to lower deceleration. Although the average operation period (110 msec) is longer than that based on general MPC, safety is guaranteed by the rule-based control running in 16 msec.

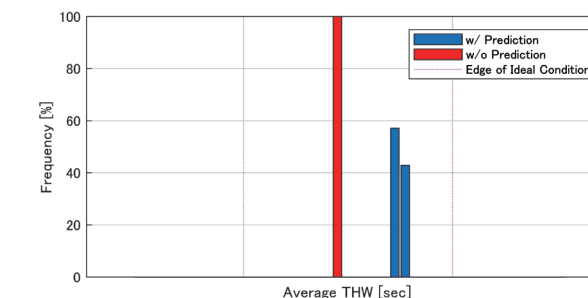


Fig. 13 Histogram of THW average value (preceding vehicle: pass)

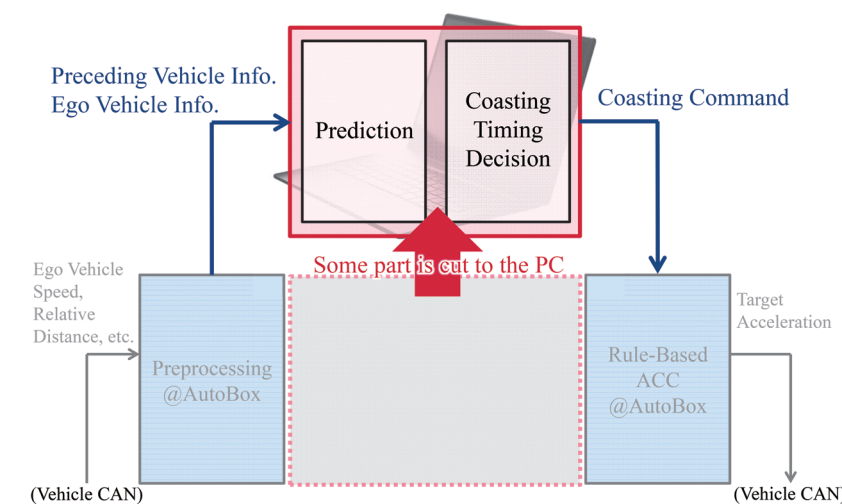


Fig. 14 Test environment implemented in actual test vehicle

6. Conclusion

In this work, a novel vehicle speed control strategy was developed to achieve both fuel economy improvement and the following function by using the prediction information with uncertainty. To realize it, a prediction technology based on IRL was introduced to predict the preceding vehicle behavior. Besides, the optimal coasting timing was determined by solving an optimization problem with the prediction information. Fuel economy improvement by the developed control strategy was validated with simulation, showing a 9.7% improvement under the condition that the ego vehicle followed the preceding vehicle before an intersection. This control strategy was implemented in an actual test vehicle to validate real-time operation.

Future issues are as follows:

- Evaluating fuel economy improvement in the real world
- Improving the prediction technology by utilizing other machine learning methods or adding various inputs derived from cameras/sensors and communication devices.

References

- 1) F. Graf, S. Lauer, S. Baensch, R. Knorr and M. Sans, "48 volt technology in the light of the connected vehicle and electrical board net advancements," In Proceedings 26th Aachen Colloquium Automobile and Engine Technology 2017, Aachen, Oct. 2017, pp. 1293-1308.
- 2) F. Flehmig, A. Sardari, U. Fischer and A. Wagner, "Energy optimal adaptive cruise control during following of other vehicles," In Proceedings 2015 IEEE Intelligent Vehicles Symposium (IV), Seoul, Jun. 2015, pp. 724-729.
- 3) M. Schori, T. J. Boehme, B. Frank and B. P. Lampe, "Optimal calibration of map-based energy management for plug-in parallel hybrid configurations: a hybrid optimal control approach," IEEE Transaction on Vehicular Technology, vol. 64, no. 9, pp. 3897-3907, 2015.
- 4) M.A.S. Kamal, S. Taguchi and T. Yoshimura, "Efficient vehicle driving on multi-lane roads using model predictive control under a connected vehicle environment," In Proceedings 2015 IEEE Intelligent Vehicles Symposium (IV), Seoul, Jun. 2015, pp. 736-741.
- 5) B. D. Ziebart, A. Maas, J. A. Bagnell and A. K. Dey, "Maximum entropy inverse reinforcement learning," In Proceedings 23rd AAAI Conference on Artificial Intelligence, Chicago, Jul. 2008, pp. 1433-1438.
- 6) M. Shimosaka, K. Nishi, J. Sato and H. Kataoka, "Predicting driving behavior using inverse reinforcement learning with multiple reward functions towards environmental diversity," In Proceedings 2015 IEEE Intelligent Vehicles Symposium (IV), Seoul, Jun. 2015, pp. 567-572.

著者



伊東 悠太郎

いとう ゆうたろう

環境ニュートラルシステム開発部
CO₂ 排出量削減技術の研究開発に従事



東谷 光晴

ひがしたに みつはる

環境ニュートラルシステム開発部
CO₂ 排出量削減技術の研究開発に従事



竹中 一仁

たけなか かずひと

先進モビリティシステム事業開発部
博士(情報理工学)
自動運転等の研究開発に従事



南條 弘行

なんじょう ひろゆき

環境ニュートラルシステム開発部
CO₂ 排出量削減技術の研究開発に従事



平野 大輔

ひらの だいすけ

先進モビリティシステム事業開発部
自動運転等の研究開発に従事